

# A serendipitous survey for galaxy clusters by the XMM-Newton Survey Science Center

A.D. Schwobe<sup>1</sup>, G. Lamer<sup>1</sup>, D. Burke<sup>2</sup>, M. Elvis<sup>2</sup>, M.G. Watson (on behalf of the XMM-SSC)<sup>3</sup>, M.P. Schulze<sup>1</sup>, G. Szokoly<sup>1,4</sup> and T. Urrutia<sup>1</sup>

<sup>1</sup>*Astrophysikalisches Institut Potsdam (AIP), An der Sternwarte 16, 14482 Potsdam, Germany*

<sup>2</sup>*Harvard-Smithsonian Center for Astrophysics, 60 Garden Street, Cambridge, MA 02138, USA*

<sup>3</sup>*X-ray Astronomy Group, University of Leicester, University Road, Leicester LE1 7RH, UK*

<sup>4</sup>*Max-Planck Institut für extraterrestrische Physik, 85748 Garching, Germany*

## ABSTRACT

We describe the initial results of a programme to detect and identify extended X-ray sources found serendipitously in XMM-Newton observations. We have analysed 186 EPIC-PN images at high galactic latitude with a limiting flux of  $1 \times 10^{-14}$  erg cm<sup>-2</sup> s<sup>-1</sup> and found 62 cluster candidates. Thanks to the enhanced sensitivity of the XMM-Newton telescopes, the new clusters found in this pilot study are on the average fainter, more compact, and more distant than those found in previous X-ray surveys. At our survey limit the surface density of clusters is about 5 deg<sup>-2</sup>. We also present the first results of an optical follow-up programme aiming at the redshift measurement of a large sample of clusters. The results of this pilot study give a first glimpse on the potential of serendipitous cluster science with XMM-Newton based on real data. The largest, yet to be fulfilled promise is the identification of a large number of high-redshift clusters for cosmological studies up to  $z = 1$  or 1.5.

## INTRODUCTION

Clusters of galaxies are the largest gravitationally bound structures in the universe and offer large diagnostic power to test cosmological models. In current scenarios of structure formation, massive clusters arise from gravitational instabilities in the extreme tail in the distribution of density fluctuations. Hence, their number density and their evolution depend critically on the initial distribution and the cosmological parameters. The number density of clusters can be used to constrain the amplitude of density fluctuations on small scales (quantified as  $\sigma_8$ ), they may be used to estimate the ratio of baryonic to non-baryonic matter in the universe from the observed baryonic fraction in clusters, and finally, to constrain the matter density,  $\Omega_0$ , by observing the number density evolution (White et al. 1993, Gheller et al. 1998, Arnaud & Evrard 1999, Wu & Xue 2000, Oukbir & Blanchard 1992, Viana & Liddle 1996, 1999, Henry 1997, Eke et al. 1998, Borgani et al. 1999, Blanchard et al. 2000).

Therefore, much effort has been spent on the definition of statistically complete samples of clusters and X-ray selection has been proven to be one of the most efficient means to build such samples. The main reasons for this are the high X-ray luminosity that allows to detect them up to redshifts  $z \simeq 1$  and beyond, and the reduced ambiguity in the identification of a cluster in the X-ray domain compared to the optical, where chance alignments play a much larger role. The first cluster samples were compiled already on the basis of UHURU, Ariel V, and HEAO-1 data (Schwartz 1978, McHardy 1978, Piccinotti et al. 1982, Kowalski et al. 1984) and comprised 76 clusters. Later on, based on the Einstein Medium Sensitivity Survey with a survey area of 740 deg<sup>2</sup>, Henry et al. (1992) established a catalog of clusters with a flux limit two orders of magnitude deeper than the non-imaging instruments could deliver with clusters reaching up to  $z = 0.58$ .

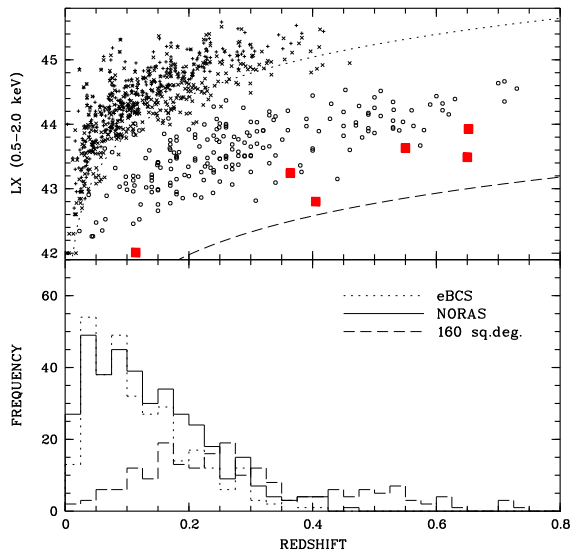


Fig. 1. The upper panel shows the distribution of galaxy clusters in the BCS (plus eBCs, + symbols), the NORAS ( $\times$ ), and the CfA 160 deg survey in the luminosity-redshift plane ( $o$ ). The lower panel shows the corresponding redshift histograms. The solid line in the upper panel indicates the sensitivity limit of the RASS. The dashed line gives a rough indication of the sensitivity limit of the survey described here. Also shown in the upper panel are the loci of six new XMM-clusters identified in the course of this programme.

Clearly, most impacting was the ROSAT mission which revealed of order 1500 X-ray selected clusters of galaxies. The search for clusters in the ROSAT data archive is still ongoing (see e.g. Cruddace et al. 2002, Böhringer et al. 2002, Ebeling et al. 2001, Rosati et al. 2002). An overview of the present knowledge of the luminosity-redshift plane of clusters is given in Fig. 1. It compares three ROSAT-based cluster surveys, the BCS (plus eBCS), the NORAS, and the CfA 160 deg<sup>2</sup> survey, sorted by increasing survey sensitivity and/or decreasing sky coverage (Ebeling et al. 1998, 2000; Böhringer et al. 2000, Vikhlinin et al. 1998). The ROSAT All-Sky Survey (RASS) with a survey area of 20391 deg<sup>2</sup> and a flux limit of  $\sim 2.4 \times 10^{-12}$  erg cm<sup>-2</sup> s<sup>-1</sup> yielded a surface density of clusters,  $N < 0.03$  deg<sup>-2</sup>. The number of high-redshift clusters,  $z > 0.4$ , is low in the RASS-based surveys and is also small in catalogues based on pointed observations. Three quarter of the Vikhlinin et al. clusters are below redshift 0.4, the faintest clusters in their survey, at  $1.6 \times 10^{-14}$ , is at about the limit of the pilot XMM-Newton based survey presented here. The MACS survey (Ebeling et al. 2001), also based on the RASS, explores the upper right corner of the  $L_x - z$  plane with considerable success. It is, however, not included in Fig. 1 since the catalogue is not yet publicly available.

XMM-Newton has the highest throughput of any imaging X-ray observatory ever flown. With its good spatial resolution, the unprecedented sensitivity of the EPIC-cameras over a wide energy range (0.5 - 12 keV) and the large field of view (30 arcmin) it detects about 50000 new X-ray sources per year serendipitously. The Survey Science Center (SSC) is a consortium of 10 European institutes with the responsibility of creating the Software Analysis System SAS, compiling the serendipitous catalogue of X-ray sources (the first version is due for release in early 2003, [http://xmmssc-www.star.le.ac.uk/newpages/xcat\\_public.html](http://xmmssc-www.star.le.ac.uk/newpages/xcat_public.html)) and carrying out a follow-up and identification programme (XID). The whole project is described by Watson et al. (2001). In the XID-programme the SSC is pursuing two closely related programmes: optical/near-IR imaging of large numbers of XMM-Newton fields, and a ‘core’ programme to spectroscopically identify a significant sample of X-ray sources. In the first phases of the programme we have concentrated mainly on the identification of point-like X-ray sources (Barcons et al. 2002, Watson et al. 2003), here we describe preliminary results of a study to characterize extended sources in XMM-Newton images. The potential of the serendipitous source content of XMM-Newton for cluster science was outlined by Romer et al. (2001).

## THE XMM-NEWTON SSC CLUSTER SURVEY

The cluster project is embedded in the overall XID project of the SSC, i.e. the software and the energy bands for the source detection are the same as for the pipeline processing of all data. The results will be made publicly available via the web-pages of the SSC. In order to test the software and to optimize the strategy for the production of a large sample of clusters, we have set up a pilot study whose results are described here.

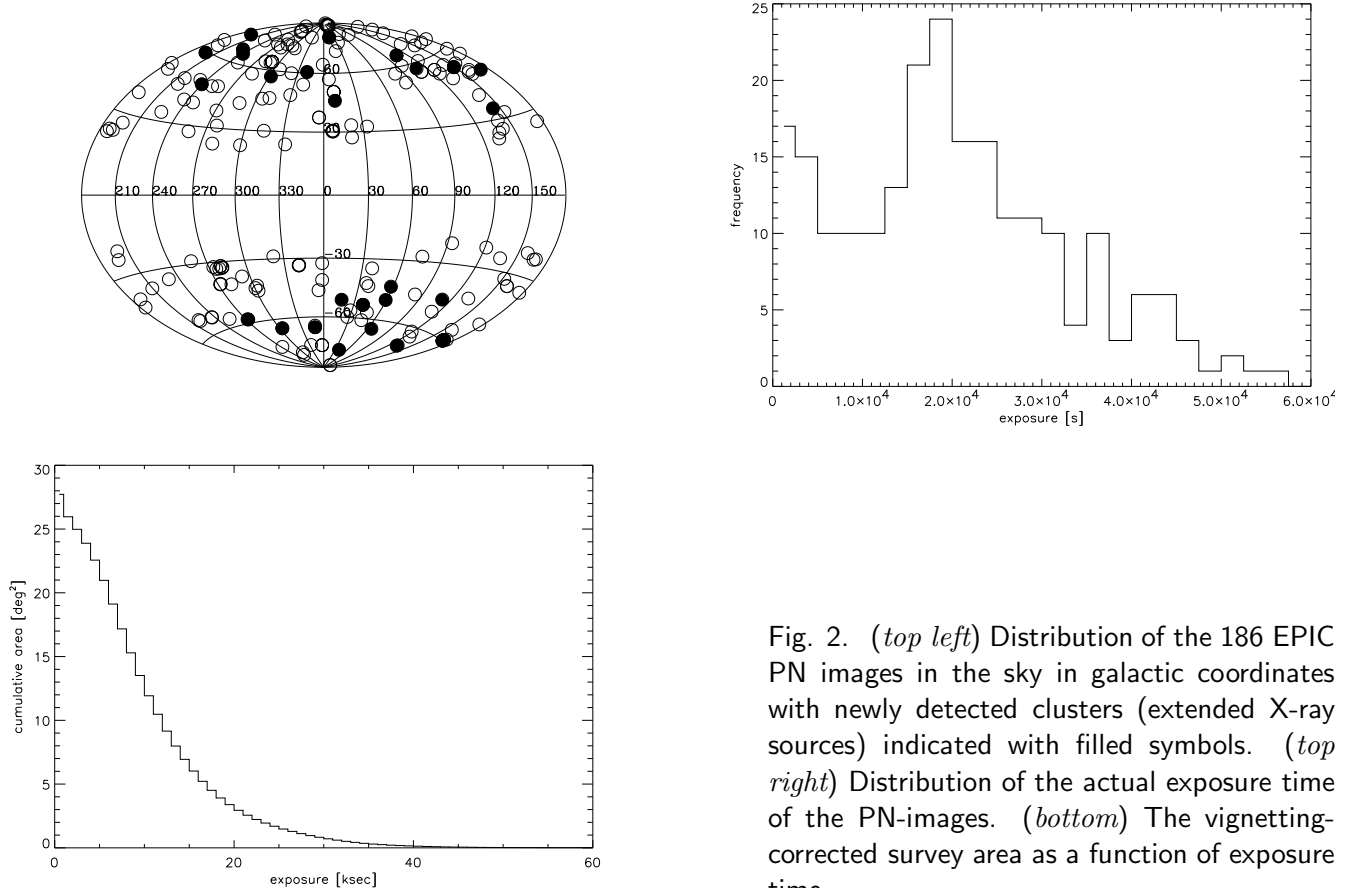


Fig. 2. (*top left*) Distribution of the 186 EPIC PN images in the sky in galactic coordinates with newly detected clusters (extended X-ray sources) indicated with filled symbols. (*top right*) Distribution of the actual exposure time of the PN-images. (*bottom*) The vignetting-corrected survey area as a function of exposure time.

### Field selection

For this pilot study we have selected observations for which the observation PI granted SSC follow-up permission. This was declared already on the original proposal forms and applies to  $\sim 75\%$  of all proposals. This permission is granted to the non-target content of the observations, hence, XMM-observations of known clusters are excluded from our pilot study. We used images from the EPIC-PN camera only with the camera being operated in the ‘FullFrame’ or the ‘LargeWindow’ mode. It is planned later to combine the PN- and MOS-images, which will help to better characterize the cluster morphology (bridging of CCD chip gaps) and the spectral shape. We restricted ourselves to fields at high Galactic latitude,  $|b| > 20^\circ$ , thus facilitating the planned optical follow-up. In order to gain in depth and to produce a tractable number of possible fields we selected observations with nominal exposure times  $> 20$  ksec. However, the time needed for the set up of the PN-CCD and the loss of time due to bad space weather lead to a significant decrease of the usable exposure time. The application of the different selection criteria led to a total of 186 EPIC PN fields which were subsequently analysed. The fields are more or less homogeneously distributed in the sky and the actual observation time stretches from 2 ksec to 60 ksec with a peak at 18 ksec (Fig. 2).

The geometric survey area of these observations is  $\sim 27.7 \text{ deg}^2$ . The integrated vignetting corrected survey area of the 186 images, taking into account only good time intervals is also shown in Fig. 2. Despite the large number of fields, the survey area at 20 ksec true exposure, i.e. at our nominal minimum exposure time, is only  $2.94 \text{ deg}^2$ , roughly a factor of 10 below the integrated geometric area.

### Source search

For each of the 186 observations, EPIC PN images were created in the XID-band between 0.5–4.5 keV. The *edetect\_chain* of XMM SAS was used to search for extended sources, and the task *emldetect* was used to fit extended model profiles to all detected sources. The source detection software combines a sliding-box detection and maximum-likelihood profile fitting with Gaussian point-spread functions (PSF). The width of the PSF is adjusted according to the off-axis angle. The thresholds for detection likelihood and extent

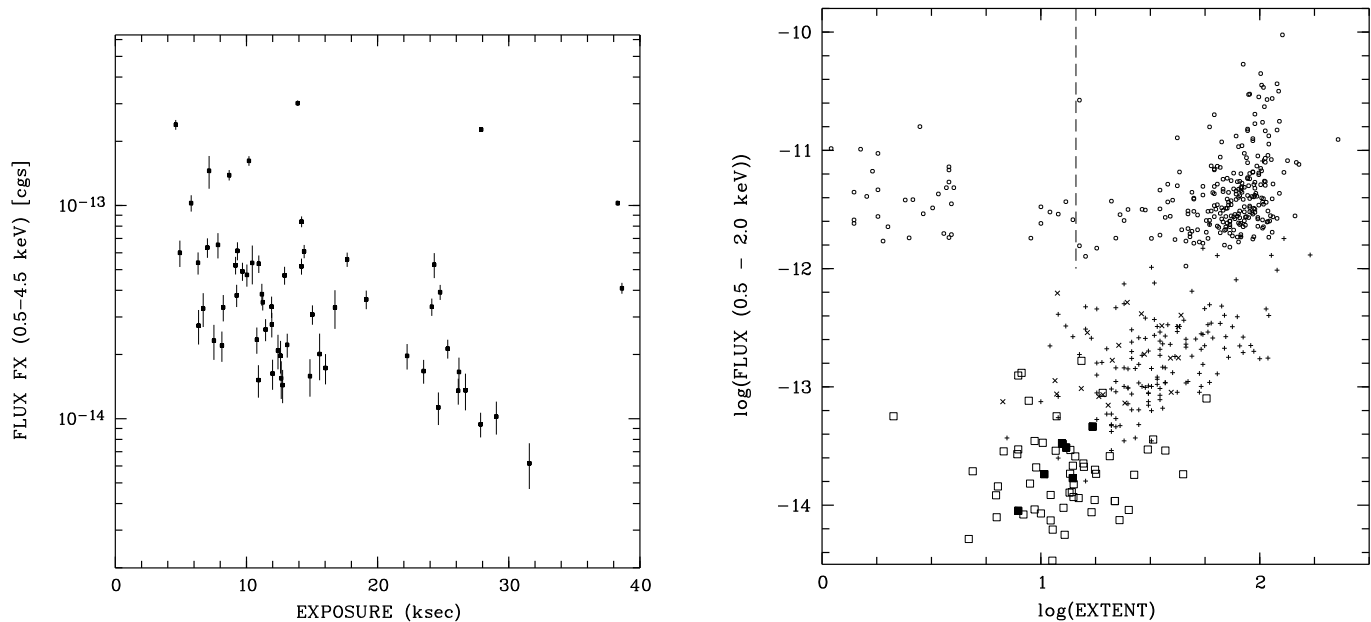


Fig. 3. (*left*) X-ray flux (0.5–4.5 keV) of cluster candidates as a function of vignetting-corrected exposure time. (*right*) Distribution of newly found XMM-clusters in the X-ray-flux/extent plane (squares, filled symbols for clusters with measured redshift) compared with clusters from the RBS ( $\circ$ ), the WARPS ( $\times$ ) and CfA 160 deg surveys ( $+$ ). The quantity plotted which describes the extent of the XMM-clusters is the Gaussian  $\sigma$ . For the ROSAT clusters the plotted quantities are: RBS – the amount by which the maximum likelihood fit is improved over a pointlike PSF ( $\sim 14$  arcsec, indicated by the vertical dashed line); WARPS & CfA 160 deg – the cluster core radius

likelihood were set to 10. The resulting fluxes of the extended sources were multiplied by a factor of 1.25, which accounts for the deviation of Gaussian-approximated cluster fluxes from the usually better fitting King profiles and was determined by detection runs on simulated PN images (Brunner & Lamer 2003). Clearly, the derived X-ray fluxes are a first approximation only, since the true cluster profile might also be different from the assumed King profile (particularly in dynamically young and irregular clusters), and since X-ray point-sources are bound to be embedded in the diffuse cluster emission. The fluxes of ROSAT clusters are typically given in the 0.5 – 2.0 keV band. For the comparison between ROSAT and XMM-Newton clusters (Figs. 1 and 3b), we applied a flux factor of 0.55, which accounts for the different energy bands. This assumes a solar-abundance Raymond-Smith spectrum of  $kT_{\text{RS}} = 4.8$  keV, absorbed by cold interstellar matter with  $N_H = 4 \times 10^{20} \text{ cm}^{-2}$ . The source lists were screened visually in order to remove spurious detections. These originate mainly from imperfect background determinations in the vicinity of CCD gaps or near bright or extended X-ray sources.

## Results

The limiting flux of the survey is  $F_{\text{lim}} \sim 10^{-14} \text{ erg cm}^{-2} \text{ s}^{-1}$  in the 0.5 – 4.5 keV band, depending on exposure and extent of the sources. At this flux limit we find 62 clearly extended X-ray sources which are regarded as cluster candidates. As expected, all new clusters are fainter than the RASS limit, the observed range is  $7 \times 10^{-15} - 2.5 \times 10^{-13} \text{ erg cm}^{-2} \text{ s}^{-1}$ . The median flux of the new clusters is  $\sim 3 \times 10^{-14} \text{ erg cm}^{-2} \text{ s}^{-1}$ . About one third of the clusters were detected in relatively shallow exposures below 10 ksec, which means that the planned full survey will make use of all suitable XMM-fields disregarding the exposure time (see Fig. 3, left). In the  $3 \text{ deg}^2$  area with true exposure in excess of 20 ksec we find 15 clusters, which corresponds to a surface density of  $5 \text{ deg}^{-2}$ , more than a factor of 100 higher than at the limit of the RASS.

The median extent of the cluster candidates is  $\sim 13''$ . In the present sample no correlation between X-ray extent and X-ray flux is obvious. The right panel of Fig. 3 compares the X-ray fluxes and X-ray extent

of the new XMM-Newton clusters with different ROSAT-based X-ray surveys (RBS - Schwobe et al. 2000, CfA 160 deg – Vikhlinin et al. 1998, WARPS – Perlman et al. 2002). Although the quantities plotted in the figures are not exactly the same for the different samples, the comparison is nevertheless instructive. The X-ray flux of the XMM-Newton clusters was transformed from the XID band (0.5 – 4.5 keV) to the ROSAT band assuming a 4.8 keV Raymond-Smith spectrum absorbed by a column with  $N_H = 4 \times 10^{20} \text{ cm}^{-2}$ . The X-ray extent of the XMM-Newton clusters is the Gaussian  $\sigma$ . The number which quantifies the extent of the RBS-clusters is the extent parameter as found in the ROSAT Bright Source catalogue by Voges et al. (1999), i.e. the Gaussian  $\sigma$  which exceeds the PSF of a pointlike source ( $\sim 14$  arcsec). RBS-clusters to the left of the dashed line in the Fig. 3b are unresolved at the ROSAT-RASS resolution. Since the ROSAT point-source PSF is small compared to the typical extent of a RBS-cluster, the quantities plotted for the XMM- and the RBS-clusters are nevertheless comparable (see the discussion of X-ray extent in the RASS by Ebeling et al. 1998). The extent parameter plotted for the WARPS and CfA 160 deg clusters is the cluster core radius as drawn from the tables in Perlman et al. (2002) and Vikhlinin et al. (1998), respectively.

There is a pronounced trend from the bright, extended RBS-clusters towards the faint, compact XMM-clusters. The median extent of the new XMM-clusters is just compatible with the PSF of a point-like X-ray source in the RASS. Thanks to the good point-spread function and sensitivity of the XMM-mirrors, faint, apparently compact X-ray selected galaxy clusters are detected and can be studied. Presently we are exploring the completeness of our cluster detection procedure. The *emldetect* task detects extended sources of size up to 1/8 of a PN CCD, i.e. up to 30 arcsec, which limits the detection of extended, low-surface brightness structures. The *ewavelet* task will be used to complement source lists in future versions of our catalogue.

### Optical identifications

Follow-up optical observations were initiated using facilities at ESO, Calar Alto, the ING at La Palma and Las Campanas. Imaging data were obtained in the framework of the optical imaging programme of the SSC, mostly with the WFC at the 2.5m INT and with the WFI at the ESO/MPG 2.2m telescope at La Silla (see [http://xmmssc-www.star.le.ac.uk/newpages/xid\\_public.html](http://xmmssc-www.star.le.ac.uk/newpages/xid_public.html)). These large-format, wide-field cameras provide photometry with limiting magnitude of  $V = 23 - 24$  mag and excellent astrometry. Follow-up low-resolution spectroscopy of about 15 cluster candidates was performed at the Magellan I telescope. Six of them belong to the sample described in this paper. We obtained long-slit spectra of the brightest cluster galaxies with the LDSS-2 and the Boller & Chivens spectrographs, and determined redshifts in the range  $z = 0.07 - 0.65$ . Fluxes and luminosities of the six new clusters in the present sample are shown in comparison with ROSAT clusters in Figs. 1 and 3b. It is obvious that the XMM-clusters extend the accessible parameter range in the  $(L_X - z)$  and  $(F_X - \sigma)$  planes.

Particularly intriguing is the discovery of paired clusters of galaxies at high redshift, thus offering direct access to the study of large-scale structures. In Fig. 4 we show a cut-out of the EPIC PN image of the field of WW Hor, observed in the CalPV phase (revolution 181) for a total of 21148 sec with Full Frame through the thin filter. The target, a cataclysmic variable star, is the bright point source in the upper part of the PN image. VLT R-band images of the two clusters are also shown in the figure. Spectra with Magellan I were taken of the brightest galaxies in each cluster which gave identical redshifts of  $z = 0.65$ . At the distance of the two clusters, their angular separation of 270 arcsec corresponds to only a few diameters of the clusters and is just  $2h_{50}^{-1}$  Mpc. There are EPIC-PN fields with a much larger number, 8 – 10, of extended sources. Whether these really form part of large-scale structures has to be tested by deep multi-color imaging and dedicated spectroscopy.

### SUMMARY AND OUTLOOK

We have presented some initial results of a programme to understand the extended source content in XMM-Newton EPIC PN images. This project demonstrates the relative ease of creating large samples of clusters of galaxies with XMM-Newton using X-ray extent as single selection criterion. The method will be particularly valuable to find a significant number of clusters at high redshift and to study cluster evolution up to redshifts of  $z \sim 1 - 1.5$ . We have shown already how the accessible parameter range in the  $F_X - \sigma$  plane is enlarged by the newly detected clusters and we should be able to enlarge the parameter range also in the  $(L_X - z)$  plane.

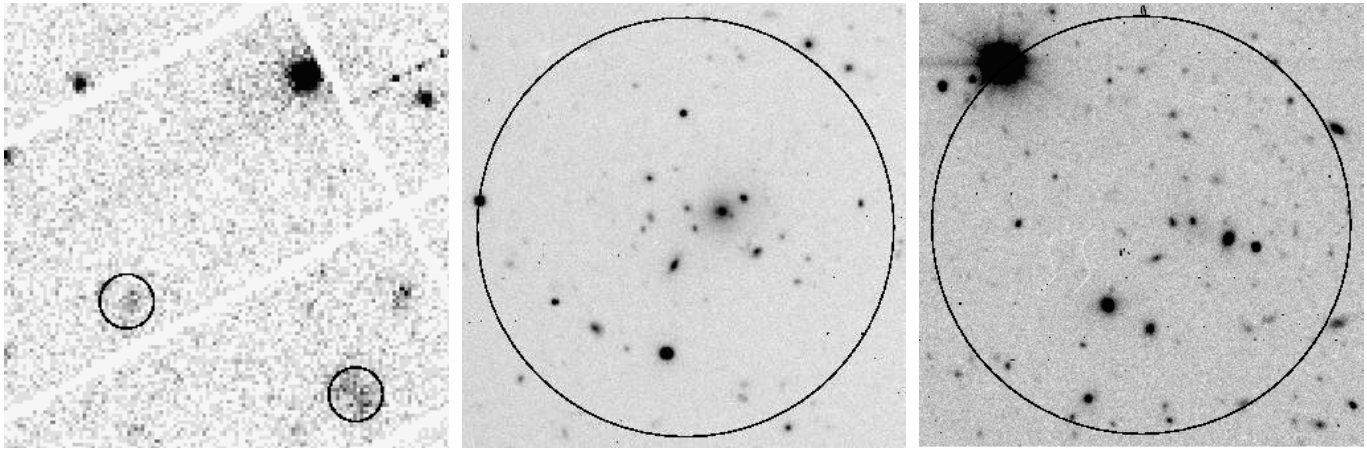


Fig. 4. EPIC-PN (left) and VLT R-band images of the cluster pair discovered in the field of WW Hor. The circles have a size of 30 arcsec in all three images. Spectra were taken of the two brightest cluster galaxies. These were found at identical redshift of  $z = 0.65$ .

Future work in the X-ray domain will concentrate on the optimisation of the source detection, the inclusion of the MOS images, and a more thorough determination of the survey area (taking into account the lack of sensitivity for extended source detection in the vicinity of bright and/or extended sources). Also more effort needs to be spent on the determination of the source parameters, like temperature, extent, and flux. The temperature of the X-ray emitting gas of the brighter clusters will be determined by proper spectral fits and will be estimated by X-ray hardness ratios for the clusters with low numbers of counts. A thorough optical observation programme has been set up in order to determine redshifts of the new clusters by photometry and spectroscopy.

#### ACKNOWLEDGEMENTS

This work is based partly on observations with XMM-Newton, an ESA Science Mission with instruments and contributions directly funded by ESA member states and the USA (NASA). This project is supported in part by the German BMBF under DLR grant 50 OX 0201. Based in part on observations performed with the ESO/WFI under programmes 68.A-0473 and 69.A-0615. We thank an anonymous referee for constructive criticism.

#### REFERENCES

- Arnaud, M. and A.E. Evrard, The  $L_X - T$  relation and intracluster gas fractions of X-ray clusters, *MNRAS*, **305**, 631A, 1999
- Barcons, X., Carrera, F.J., Watson, M.G., McMahon, R.G., Aschenbach, B., Freyberg, M.J., Page, K., Page, M.J., Roberts, T.P., Turner, M.J.L., et al., The XMM-Newton serendipitous survey. II. First results from the AXIS high galactic latitude medium sensitivity survey, *A&A*, **382**, 522, 2002
- Blanchard, A., Sadat, R., Bartlett, J.G., and M. LeDour, A new local temperature distribution function for X-ray clusters: cosmological applications, *A&A*, **362**, 809, 2000
- Böhringer, H., Collins, C.A., Guzzo, L., Schuecker, P., Voges, W., Neumann, D.M., Schindler, S., Chincarini, G., De Grandi, S., and R.G. Cruddace et al., The ROSAT-ESO Flux-limited X-Ray (REFLEX) Galaxy Cluster Survey. IV. The X-Ray Luminosity Function, *ApJ*, **566**, 93, 2002
- Böhringer H., Voges W., Huchra J.P., McLean B., Giacconi R., Rosati P., Burg R., Mader J., Schuecker P., Simic D., Komossa S., Reiprich T.H., Retzlaff J., Trümper J., The northern ROSAT all-sky (NORAS) galaxy cluster survey. I. X-ray properties of clusters detected as extended X-ray sources. *Astrophys. J. Suppl. Ser.* **129**, 435 (2000)
- Borgani, S., Girardi, M., Carlberg, R.G., Yee, H.K.C., and E. Ellingson, Velocity Dispersions of CNOCClusters and the Evolution of the Cluster Abundance, *ApJ*, **527**, 561, 1999
- Brunner, H., and G. Lamer, Performance of the X-ray source detection package within the XMM-Newton

- Standard Analysis System, Proc. *New visions of the X-ray Universe*, in press, 2003
- Cruddace, R., Voges, W., Böhringer, H., Schuecker, P., Ebeling, H., and S. De Grandi, The ROSAT All-Sky Survey: a Catalog of Clusters of Galaxies in a Region of 1 steradian around the South Galactic Pole, *ApJS*, **140**, 239, 2002
- Ebeling, H., Edge, A., Henry, J.P., MACS: A quest for the most massive galaxy clusters in the universe, *ApJ*, **553**, 668, 2001
- Ebeling, H., Edge, A., Böhringer, H., Allen, S.W., Crawford, C.S., Fabian, A., Voges, W., and J.P. Huchra, The ROSAT Brightest Cluster Sample-I. The compilation of the sample and the cluster  $\log N - \log S$  distribution, *MNRAS*, **301**, 881, 1998
- Ebeling H., Edge A.C., Böhringer H., Allen S.W., Crawford C.S., Fabian A.C., Voges W., Huchra J.P., The ROSAT brightest cluster sample - I. The compilation of the sample and the cluster  $\log N - \log S$  distribution. *Mon. Not. R. Astron. Soc.*, **301**, 881 (1998)
- Ebeling H., Edge A.C., Allen S.W., Crawford C.S., Fabian A.C., Huchra J.P., The ROSAT Brightest Cluster Sample - IV. The extended sample. *Mon. Not. R. Astron. Soc.*, **318**, 333 (2000)
- Eke, V.R., Navarro, J.F., and C.S. Frenk, The Evolution of X-Ray Clusters in a Low-Density Universe, *ApJ*, **503**, 569, 1998
- Gheller, C., Pantano, O., and L. Moscardini, Constraining the cosmological baryon density with X-ray clusters, *MNRAS*, **296**, 85, 1998
- Henry, J.P., A measurement of the density parameter derived from the evolution of cluster X-Ray temperatures, *ApJ*, **489**, 1, 1997
- Henry, J.P., Gioia, I.M., Maccacaro, T., Morris, S.L., Stocker, J.T., and A. Wolter, The extended medium sensitivity survey distant cluster sample - X-ray data and interpretation of the luminosity evolution, *ApJ*, **386**, 408, 1992
- Kowalski, M.P., Cruddace, R.G., Wood, K.S., and M.P. Ulmer, An X-ray survey of cluster of galaxies, IV - A Survey of southern clusters and a compilation of upper limits for both Abell and southern clusters, *ApJ*, **65**, 403, 1984
- McHardy, I.M., The structure and properties of 4C radio sources in Abell clusters-II. The declination ranges 10-20 and 50 degrees, *MNRAS*, **815**, 927, 1978
- Oukbir, J., and A. Blanchard, X-ray clusters in open universes, *A&A*, **262L**, 201, 1992
- Perlman E.S., Horner D.J., Jones L.R., Scharf C.A., Ebeling H., Wegner G., Malkan M., The WARPS Survey: VI. Galaxy Cluster and Source Identifications from Phase I. *ApJS*, **140**, 265
- Piccinotti, G., Mushotzky, R.F., Boldt, E.A., Holt, S.S., Marshall, F. E., Serlemitsos, P. J., and R.A. Shafer, A complete X-ray sample of the high-latitude sky from HEAO 1 A-2 -  $\log N - \log S$  and luminosity functions, *ApJ*, **253**, 485, 1982
- Romer, A.K., Viana, P.T.P., Liddle, A.R., and R.G. Mann, A Serendipitous Galaxy Cluster Survey with XMM: Expected Catalog Properties and Scientific Applications, *ApJ*, **547**, 594, 2001
- Rosati, P., Borgani, S., and C. Norman, The Evolution of X-ray Clusters of Galaxies, *ARA&A*, **40**, 539, 2002
- Schwartz, D.A., The X-ray luminosity function of Abell clusters, *ApJ*, **220**, 8, 1978
- Schwope, A.D., Hasinger, G., Lehmann, I., et al., The ROSAT Bright Survey: II. Catalogue of all high-galactic latitude RASS sources with PSPC countrate  $CR > 0.2s^{-1}$ , *Astron. Nachr.*, **321**, 1, 2000
- Viana, P.T.P., and A.R., Liddle, The cluster abundance in flat and open cosmologies, *MNRAS*, **281**, 531, 1996
- Viana, P.T.P., and A.R., Liddle, Galaxy clusters at  $0.3 < z < 0.4$  and the value of  $\Omega_0$ , *MNRAS*, **303**, 535, 1999
- Vikhlinin A., McNamara B.R., Forman W., Jones C., Quintana H., Hornstrup A., A catalog of 200 galaxy clusters serendipitously detected in the ROSAT PSPC pointed observations, *Astrophys. J.* **502**, 558 (1998)
- Watson, M. G., Augueres, J.-L., Ballet, J., et al., The XMM-Newton Serendipitous Survey I. The role of XMM-Newton Survey Science Centre, *A&A*, **365**, L51, 2001
- Watson, M.G., Pye, J.P., Denby, M., et al., The XMM-Newton serendipitous source catalogue. *AN*, **324**, 89
- Wu, X.P., and Y.-J. Xue, Constraints on the asymptotic baryon fractions of galaxy clusters at large radii, *MNRAS*, **311**, 825, 2000
- White, S.D.M., Efstathiou, G., and C.S. Frenk, The amplitude of mass fluctuations in the universe, *MNRAS*,

**262**, 1023, 1993

E-mail address of A.D. Schwope [aschwope@aip.de](mailto:aschwope@aip.de)